acta physica slovaca vol. 51 No. 5, 271 – 279 **October 2001**

PREEQUILIBRIUM DECAY IN ALPHA PARTICLE INDUCED REACTIONS IN TERBIUM

N. L. Singh, M. S. Gadkari
Physics department, Faculty of Science, M. S. University of Baroda, Vadodara - 390 002,India

Received 25 June 2001, in final form 4 September 2001, accepted 6 September 2001

The excitation functions of ^{159}Tb[(α,n), (α,3n), (α,4n), (α,α3n) reactions were measured using stacked foil activation technique and HPGe gamma ray spectroscopy method up to 50 MeV. The experimental results were compared with the theoretical predictions considering equilibrium as well as preequilibrium contributions using code ALICE/90. It was found that the initial exciton configuration n_0 = 4(4p0h) that is pure particle state , appears to give good fit to the experimental data.

PACS: 25.60.Dz

1 Introduction

There is increasing experimental evidence pointing out to new types of processes that lie in complexity between the one shot direct interaction and the many body compound nucleus processes. In the new perspective, it is assumed that the projectile-target composite system is characterised by a few degrees of freedom of the first interaction and passes through a series of intermediate stages of increasing complexity, and reaches the final stage of a compound nucleus having a statistical equilibrium with a large number of degrees of freedom.

In order to explain the physics of nuclear equilibration, several semiclassical preequilibrium reaction models have been developed to explain a wide range of charged particle spectra and excitation functions induced by alpha particles in the energy region of 20-200 MeV. Most of these models utilise one way or another the two basic concepts developed in the Intranuclear Cascade (INC) Model of Goldberger [1] and the Statistical Model of Intermediate Structure (SMIS) first proposed by Griffin [2]. As a result, a number of formulations, the hybrid model [3], the exciton model [4] and many other models [5,6,7] have emerged as descendents of Griffin's statistical model of intermediate structure, which is also loosely called as Griffin's "exciton model". Thus in recent years, there have been far reaching improvements in the semiclassical models and they are often used for making comparison with experimental results, on account of their simplicity and transparency. Not only the validity of these models have been extended up to a few hundreds of MeV in excitation, but also the important influence of multiparticle emission in the preequilibrium mode have been incorporated into the model frame work. Blann[3], who is continuously improving his computer code based on hybrid model, in 1984, introduced new algorithms into

the code ALICE/85/300 [8] to calculate the preequilibrium multinucleon emission in an approximate way. Later on, Kataria et al [9] have incorporated a shell dependent level density formula of Kataria, Ramamurthy and Kapoor [10] into the above code, which takes into account the effect of nuclear shell structure on level densities of residual nuclei. This modified code is known as ALICE/90 [9].

Terbium is a typical monoisotopic element belonging to rare earth group. The study of excitation functions for (α,xn) reactions on terbium gives information about the preequilibrium reaction mechanism. In the region of excitation energy between 20-50 MeV, gradually the preequilibrium reaction mechanism predominates over the compound nucleus mode. It is important to assess the influence of preequilibrium emission, more and more experimental data are needed. With this motivation, the present work is undertaken to study the excitation functions of four reactions induced by alpha particles on ^{159}Tb up to 50 MeV.

2 Experimental details

The excitation functions for alpha particle induced reactions on terbium were studied by the stacked foil activation technique and High Purity Germanium (HPGe) gamma ray spectroscopy method. Spectroscopically pure (99.99%) terbium foils of thickness 20.6 mg/cm^2 were used as the target. The samples were cut into pieces of 1.2 $\times$ 1.2 cm^2 each and glued on aluminium frame of size 3.0 $\times$ 2.5 cm^2 having a circular hole of diameter 8mm in its centre. The aluminium foils of varying thickness were also inserted in the stack, which acts as energy degraders. As the beam passes through the successive foils of the stack, the alpha beam looses its energy but not the intensity. Hence each experimental foil sees effectively a beam of different energy falling on it. The energy of the alpha beam after they had traversed half the thickness of each foil was computed from the range-energy tables [11].

The irradiations were carried out at Variable Energy Cyclotron Centre (VECC), Calcutta, India. The beam spot on the foil stack was restricted to 5.00 mm by a central hole in a 6.00 mm thick tantalum collimator placed in front of the stack. The alpha beam were totally stopped in the electrically insulated irradiation head serving as a kind of Faraday Cup, where secondary electrons were prevented from escaping [12,13]. The total thickness of the stack was chosen to be definitely less than the range of the alpha particle beam in the materials of the stack. A beam current of the order of 200 nA was used . During the irradiation, a low conductivity water (LCW) is circulated through specially designed jet assembly, which cooled both the flange as well as the stack. The incident alpha particle flux was calculated by measuring the activities of ^{27}Al (α,α2pn)^{24}Na, for which well measured cross sections are available in the literature [14]. The charge collected in the Faraday Cup was also used to calculate the average incident α-beam flux. In general, the two values agreed within 5%. The activities produced in each foil were measured using a 120 cc HPGe detector, having a resolution of 2.0 keV for 1332 keV photons, in conjunction with a 4096 channels multichannel analyser. The residual nuclei were identified and their yields measured using their characteristic gamma rays mentioned in Table I [15]. In general, several gamma rays arising from the same residual nucleus have been identified.

The dead time for counting has been kept less than 5% by adjusting the sample-detector distance in this measurement and proper care has been taken in the calculations. As a ckeck in some cases, the relative intensities of the identified gamma rays were also measured and found to

Table I. Nuclear data used for identification of residual nuclei [15].

REACTION	Q-VALUE (MeV)	$T_{1/2}$	E_γ (keV)	θ_γ (%)
^{159}Tb(α,n)^{162m}Ho	-9.4	68m	185	29.0
			283	14.5
			937	13.8
^{159}Tb(α,n)^{162}Ho	-9.1	15m	81	7.7
			1319	3.7
^{159}Tb(α,3n)^{160m}Ho	-24.9	5.02h	728	29.7
			962	17.6
			966	16.2
^{159}Tb(α,3n)^{160}Ho	-24.99	26m	728	29.7
			962	17.6
			966	16.2
^{159}Tb(α,4n)^{159}Ho	-32.0	33m	121	34.0
			132	22.7
			253	14.0
			310	14.4
^{159}Tb(α,α3n)^{156}Tb	-23.6	5.4d	199	41.8
			534	66.2
			1222	31.7
Monitor Reaction ^{27}Al(α,α2pn)^{24}Na	-31.4	15.05h	1369	100.0

agree well with the literature values [15]. The cross sections were determined from the observed intensities of the various gamma rays originating from the same residual nucleus and finally their weighted average was taken. The energy calibration and the efficiency of the detector were determined with a ^{152}Eu standard source. The formula used for the determination of cross section was reported in our earlier paper [16].

3 Results and discussion

3.1 Experimental errors

The overall errors in the presently measured cross sections are subdivided in to the following categories.

(i) In order to estimate the number of nuclei in the sample and to check the thickness and uniformity of the sample, pieces of sample foils of different dimensions were weighted on an electronic microbalance and the thickness of each foil was calculated. This non-uniformity in the foil thickness introduces 1 to 2% error (δ_1).

(ii) Variation in the incident α-particle flux introduces some uncertainty in the final calculation of the cross sections. In the present experiment the standard monitor cross sections were taken from literature [14] in the flux determination. This introduces an overall error of 6% (δ_2).

(iii) The calculated detection efficiency may be inaccurate owing to the uncertainty in the spectroscopic data of the standard source and the statistical errors in the counts. No corrections were applied for the uncertainty in the spectroscopic data. However, the statistical error in the counting of the standard ^{152}Eu gamma source used for the efficiency calculation was estimated to be around 3-4% (δ_3).

(iv) The dead time in the pulse processing electronics lead to a loss of counts. The sample-detector distance was suitably adjusted to keep the dead time low (<5%) and corrections for it where applied accordingly in the counting rates. However, the error introduced in the determination of photopeak areas of the characteristic gamma rays were within the limits of 1 to 4% in the best and worst cases (δ_4). Therefore the total absolute error in the measured cross section is

$$\sqrt{\sum_{i=1}^{4}(\delta_i)^2}$$

and found to vary between 7 to 9% for the best and the worst cases. The above mentioned errors in the measurement of experimental cross sections do not include the uncertainty of the nuclear data (e.g. half lives of residual nuclei, branching ratio etc.) that were taken from the table of isotopes [15].

Other factors which may influence the cross section measurements are as follows :
(i) In the irradiation experiment, the initial beam energy was degraded down to around 20 MeV. As the α-beam traverses the stack material, the initial beam intensity may be disturbed.

This decrease in beam intensity introduce certain errors. The beam intensity decreases as a function of the traversed foil thickness in a stack according to the expression [12]

$$I = I_0 exp(-\sigma N_s)$$

where I_0 is the flux on the first foil , I is the flux on the last foil, σ is the total reaction cross section and N_s is the number of nuclei per unit area with reference to the entire thickness of the stack. For the experimental foil stack, N_s is given by sum of the thicknesses of the foils of the target element (T), aluminium degraders and monitor, i.e. $N_s = N_{\rm T} + N_{\rm al}$. For σ=2 barns, the maximum beam loss at the end of the stack is always less than 0.3% and hence it is neglected.
(ii) Straggling effect introduces some errors but are neglected because for alpha particles, the energy straggling at the end of the stack is always much smaller than the energy of the beam in the target foil itself. It was pointed out by Ernst et al [12] that a large number of low energy neutrons may be released as the beam traverses through the stack of foils and this in turn may disturb the yield mainly through (n,p), (n,α) reactions. However, this disturbed yield is also negligible.

3.2 Excitation functions for α-induced reaction on Terbium

The measured cross sections for the reactions ^{159}Tb(α,n)^{162m}Ho, ^{159}Tb(α,3n)^{160m}Ho, ^{159}Tb(α,4n)^{159}Ho and ^{159}Tb(α,α3n)^{156}Tb have been listed in Table II. The ^{162}Ho residual nucleus produced through Tb (α,n) reaction exists in two states. The metastable state ($T_{1/2}$=68m)

Table II. Cross sections of the α-induced reactions on ^{159}Tb.

Reaction	^{159}Tb(α,n)	^{159}Tb(α,3n)	^{159}Tb(α,4n)	^{159}Tb(α,α3n)
Product Nucleus	^{162}Ho	^{160}Ho	^{159}Ho	^{156}Tb
Threshold Energy (MeV)	9.4	25.5	32.8	24.1
E_α (MeV)	σ (mb)	σ (mb)	σ (mb)	σ (mb)
15.5 ± 1.5	16.8 ± 1.1			
21.5 ± 1.7	38.5 ± 2.7			
27.1 ± 1.1	16.6 ± 1.2	119.9 ± 8.1		
31.5 ± 0.9	10.3 ± 0.8	1045.4 ± 71.0		
35.5 ± 0.9	7.3 ± 0.5	1285.0 ± 87.3	27.1 ± 1.8	
39.4 ± 0.9	5.3 ± 0.3	633.1 ± 43.0	485.8 ± 34.0	1.1 ± 0.0
43.0 ± 0.8	4.5 ± 0.3	310.3 ± 21.1	1049.7 ± 71.3	2.4 ± 0.1
46.4 ± 0.5	3.9 ± 0.3	203.2 ± 13.8	1195.0 ± 81.2	4.4 ± 0.3

decays through isomeric transition (61%) to the ground state ($T_{1/2}$=15m) and remaining 39% through electron capture and β^+-ray emission.

In the present work, cross sections were measured for 162mHo residual nucleus. The product nucleus ^{160}Ho produced through Tb(α,3n) reaction exists in two states. The metastable state ($T_{1/2}$=5.02h) decays through isomeric transition (65%) and electron capture alongwith β^+-decay (35%). Decay of ground state ($T_{1/2}$=25.6m) is mostly through electron capture (99.6%). We have measured the cross section for ^{160m}Ho residual nucleus in the present work.

The metastable state ^{159m}Ho ($T_{1/2}$=8.3s) formed in the ^{159}Tb(α,4n) ^{159}Ho reaction decays completely through isomeric transition (100%) to ^{159g}Ho ($T_{1/2}$=33m). The activities were measured after the complete decay of metastable states to the ground state. 156Tb residual nucleus produced through ^{159}Tb(α,α3n) reaction, exists in two isomeric states of half lives 5.0h (metastable state) and 5.3d(ground state) respectively. The metastable state ^{156m}Tb ($T_{1/2}$=5.0h) decays completely through isomeric transition (100%) to ground state ^{156g}Tb ($T_{1/2}$=5.3d). The measurements were done after the complete decay of the metastable state to the ground state.

4 Comparison with theoretical predictions

The observed excitation functions for the reactions (α,xn) show the high energy tail followed by the compound nucleus formation. Therefore, the experimental cross sections may be compared with theoretical excitation functions calculated by means of the statistical model with and without the inclusion of pre-equilibrium emission of particles. We have used the code ALICE/90 [9]for the theoretical predictions.

In the pre-equilibrium part, the calculation starts with initial exciton number, i.e., particles above and holes below the fermi level induced by primary interaction and proceeds to states with increasing exciton number. The emission probability of the particles for each of these states are calculated and finally the integrated spectra yield the cross sections for the individual reactions.

Owing to the semi-classical nature, the hybrid model involves a large number of physical as well as few adjustable parameters. The model predictions of course depend on the input values given to these parameters. A short description of the options chosen is given below: The

nuclear masses were calculated from the Myers-Swiatecki mass formula [17] considering the liquid drop with shell correction without pairing i.e. the level density pairing absorbed in binding energies. The inverse cross sections were calculated from optical model subroutine included in the code. A level density parameter $a = A/9$ MeV^{-1} was used. In a priori formulation of the hybrid model, the intra nuclear transition rates are calculated either from the imaginary part of the optical model or from the free nucleon - nucleon scattering cross sections. However, for particle energies exceeding 55 MeV the optical model parameters of Becchetti and Greenless [18] are no longer applicable and thus at higher energies the mean free path for intra-nuclear transitions must be calculated from the nucleon - nucleon scattering cross sections. The mean free path multiplier 'K' was kept equal to unity. The mean free path, which is a kind of free parameter, was introduced by Blann [19] to account for the transparency of nuclear matter in the lower density nuclear periphery. The equilibrium part was calculated using standard Weisskopf and Ewing [20] formalism. It is customary to use the initial exciton number $n_0(p_0h_0)$ as a fit parameter to match the theoretical predictions with experimentally observed shape of spectra and excitation functions. It governs the entire cascading process of binary collisions and thereby influences the shape of the hard component in the particle spectrum. A good guess would be the number of nucleons in the projectile or an additional particle/hole or both [16, 21-23]. This view is quite consistent with the basic physics of preequilibrium phenomena that only a few degrees of freedom is excited in nuclear reactions at moderate energies. For the incident α-particle used in the present work, reasonable choice for the initial exciton number is n_0=4(4p0h), n_0=5(5p0h), and n_0=6(5p1h) as the initial exciton configurations. We performed the calculations using above exciton configurations and it was found that n_0=4(4p0h) gives by far the best results beyond the compound nucleus peak than the other two configurations. The predictions of n_0=5(5p0h) and n_0=6(5p1h) configurations were lower than those of n_0=4(4p0h). This is also in agreement of findings of Ernst et al[24], Blann and Komoto[25] Djalaeis et al [26], Michael and Brinkman [27] , Gadioli el al [28].

Figs. 1 and 2 show the excitation functions for Tb(α,n), Tb(α,3n), Tb(α,4n), and Tb(α,α3n) reactions with the theoretical calculations based on Weisskopf-Ewing (W.E.) estimates giving compound nucleus contributions as well as hybrid model predictions. It is observed that the W.E. estimates accounted well the low energy compound nucleus dominated part of the excitation function but failed to account for the observed high energy tail at high energies where non equilibrium effects predominate beyond a few tens of MeV of bombarding energy. The high energy region of the excitation function is accounted well by hybrid model predictions using initial exciton configuration n_0=4(4p0h), i.e. pure particle state. The threshold energies for the Tb(α,4n) and Tb(α,α3n) reactions are rather large (i.e. 32.8 and 24.1 MeV) and as such there are only a few data points in the initial rising part of the experimental excitation function. In this region the preequilibrium model predictions are not very sensitive as the compound nucleus mechanism dominates.

5 Conclusions

Excitation functions for Tb[(α,n); (α,3n); (α,4n); (α,α3n)] reactions were studied up to 50 MeV. From an overall comparison between experimental results and theoretical predictions based on compound nucleus Weisskopf-Ewing estimates as well as preequilibrium hybrid model, one can

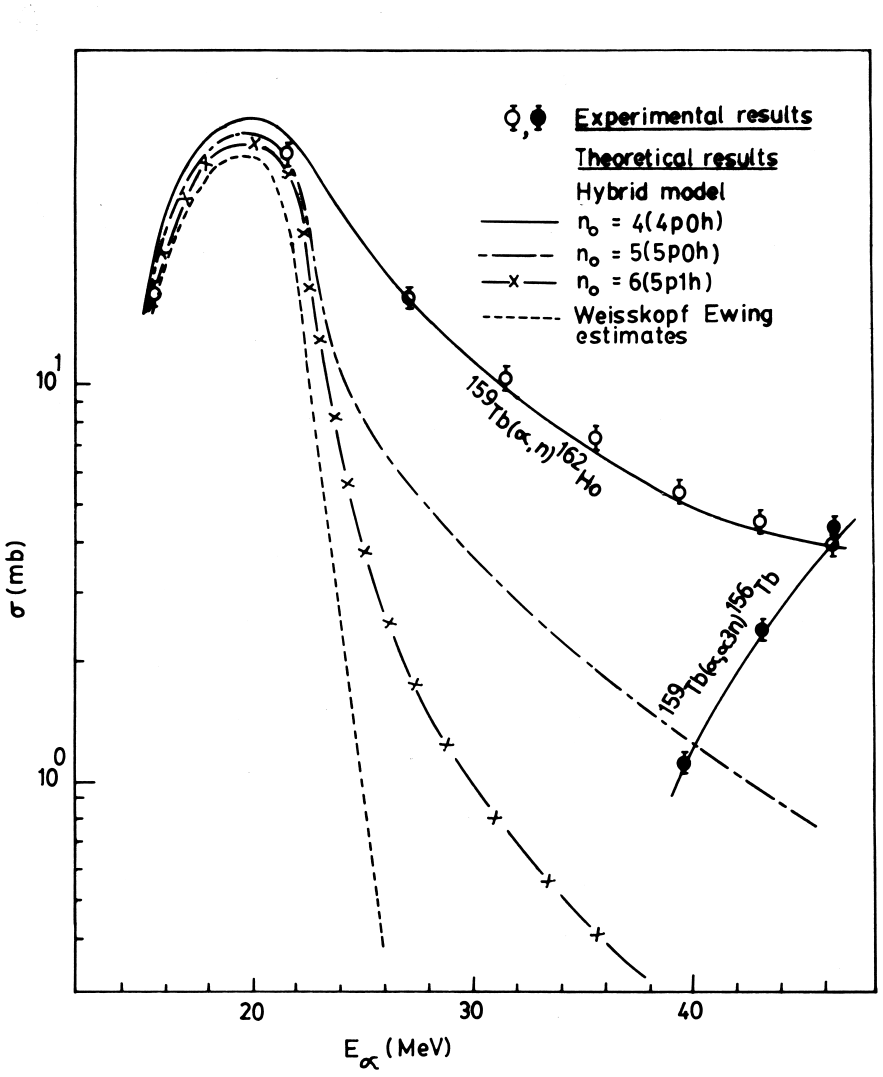

Fig. 1. Experimental and theoretical excitation functions of ^{159}Tb(α,n)^{162}Ho and ^{159}Tb(α,α3n)^{156}Tb reactions.

infer that Weisskopf-Ewing estimates accounted fairly well the low energy compound nucleus dominated part of the excitation functions but failed to account the observed cross sections at higher energies, where non-equilibrium effects predominate beyond a few tens of MeV of bombarding energy.

The hybrid model gives a fairly good account of nucleon emission with an initial exciton number n_0=4(4p0h), which is separated in the case of proton and neutron excitons (n_p and n_n

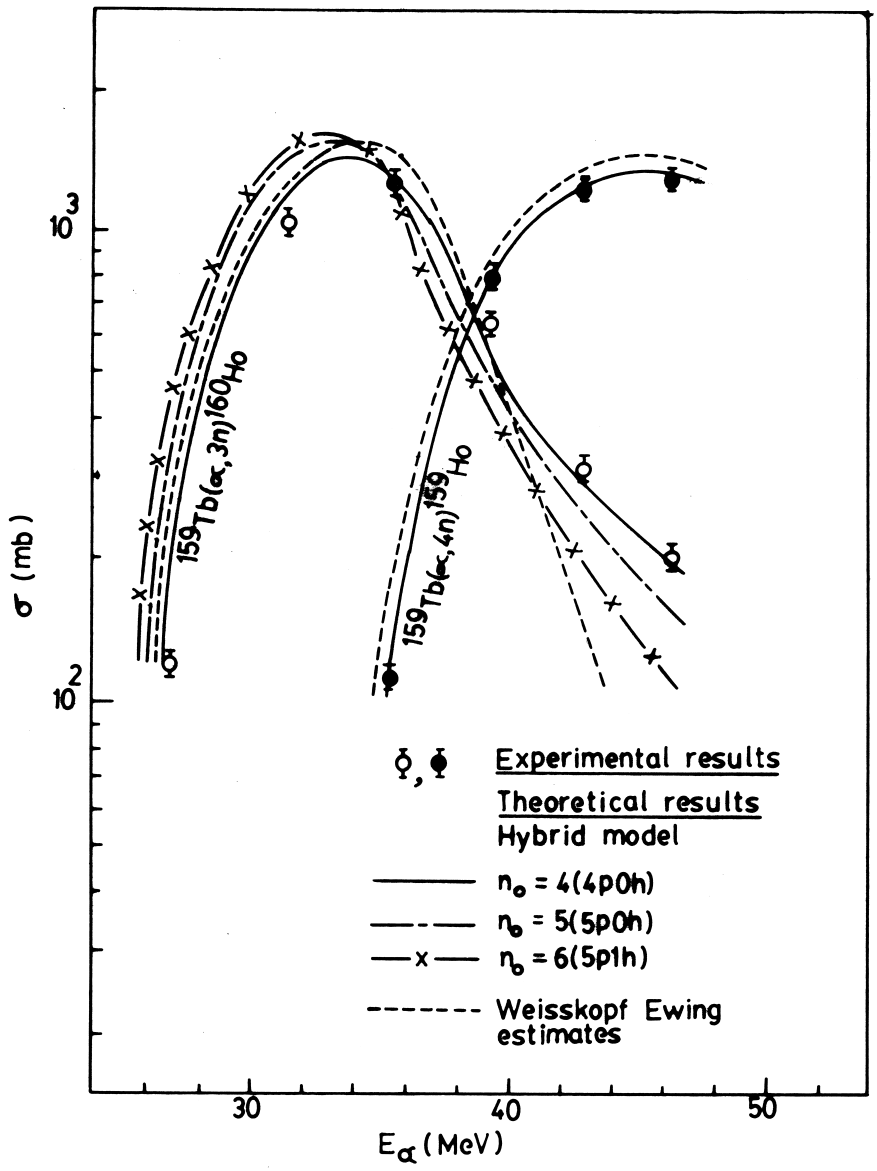

Fig. 2. Experimental and theoretical excitation functions of ^{159}Tb(α,3n)^{160}Ho and ^{159}Tb(α,4n)^{159}Tb reactions.

respectively) above and hole (n_h) below the fermi level, and the best fit is obtained with $n_p = 2$, $n_n = 2$, and $n_h = 0$ that is pure particle state. This picture is quite consistent with the basic physics of preequilibrium decay that only a small number of degrees of freedom are initially excited in a nuclear reaction at moderate energies.

Acknowledgement: The authors are thankful to the entire staff of Inter University Consortium for Department of Atomic Energy Facilities (IUC-DAEF), Calcutta Centre and Variable Energy Cyclotron Centre, Calcutta, India for their efforts in successful completion of experimental programme. The financial support by IUC-DAEF Calcutta Centre is gratefully acknowledged.

References

[1] M. L. Goldberger: *Phys. Rev.* **74** (1948) 1269
[2] J. J. Griffin: *Phys. Rev. Lett.* **17** (1966) 478
[3] M. Blann, H. K. Vonach: *Phys. Rev. C* **28** (1983) 1475
[4] E. Gadioli, E. Gadioli - Erba, P. G. Sona: *Nucl. Phys. A* **217** (1973) 589
[5] H. Machner: *Phys. Rep.* **127** (1985) 309
[6] E. Běták, J. Dobeš: *Z. Phys. A* **279** (1976) 319
[7] C. K. Cline: *Nucl. Phys. A* **210** (1973) 590
[8] M. Blann: Code ALICE/85/300, :*Lawrence Livemore National Laboratory Report UCID-20169 unpublished (1984)*
[9] S. K. Kataria, V. S. Ramamurthy, M. Blann, T. T. Komoto: Nucl. Instru. & Meth. A **288** *(1990) 585*
[10] S. K. Kataria, V. S. Ramamurthy, S. S. Kapoor: Phys. Rev. C **18** *(1978) 549*
[11] C. E. Williamson, J. P. Boujot, J. Picard: CENS report, CEA-R (1966) 3042
[12] J. Ernst, R. Ibowski, H. Klampfl, H. Machner, T. Mayer- Kuckuk, R. Schanz: Z.Phys. A **308** *(1982) 301*
[13] N. L. Singh, S. Mukherjee, D. R. S. Somayajulu: Nuovo Cimento Soc. Ital. Fis.A **107** *(1994) 1635*
[14] H. J. Probst, S. M. Qaim, R. Weinreich: Int. J. App. Rad. Isotopes **27** *(1976) 431*
[15] C. M. Lederer, V. S. Shirley: Table of Isotopes, 7th edition (Eds. John Wiley & sons) New York (1978)
[16] M. S. Gadkari, H. B. Patel, D. J. Shah, N. L. Singh: Physica Scripta 55 **1997** *(147)*
[17] 17. W. D. Myers, W. J. Swiatecki: Ark. Fys. **36** *(1967) 343*
[18] F. D. Becchetti, F. W. Greenless: Phys. Rev. **182** *(1969) 1190*
[19] M. Blann: Phys. Rev. Lett. **27** *(1971) 337*
[20] V. F. Weisskopf, D. H. Ewing: Phys. Rev. **57** *(1940) 472*
[21] N. L. Singh, M. S. Gadkari, S. N. Chintalapudi: Physica Scripta **61** *(2000) 550*
[22] N. L. Singh, S. Mukherjee: Acta Physica Slovaca **48** *(1998) 469*
[23] S. Mukherjee, A. K. Sharma, D. Bakhru, N. L. Singh: Physica Scripta **58** *(1998) 319*
[24] J. Ernst, W. Friedland, H. Stockhorst: Z. Phys. A **27** *(1976) 145*
[25] M. Blann, T. T. Komoto: Phys. Rev. C **29** *(1984) 1678*
[26] A. Djalaeis, P. John, H. J. Probst, C. M. Boricke: Nucl. Phys. A **250** *(1975) 149*
[27] R. Michel, G. Brinkmann: Nucl. Phys. A **333** *(1980) 167*
[28] E. Gadioli, E. Gadioli - Erba, J. J. Hogan: Phys. Rev. C **16** *(1977) 1404*